

# A novel mode of DnaA–DnaA interaction promotes ADP dissociation for reactivation of replication initiation activity

Ryo Sugiyama<sup>1,†</sup>, Kazutoshi Kasho<sup>1,†</sup>, Kenya Miyoshi<sup>1</sup>, Shogo Ozaki<sup>1</sup>, Wataru Kagawa<sup>2</sup>, Hitoshi Kurumizaka<sup>3</sup> and Tsutomu Katayama<sup>1,\*</sup>

<sup>1</sup>Department of Molecular Biology, Graduate School of Pharmaceutical Sciences, Kyushu University, Higashi-ku, Fukuoka 812-8582, Japan, <sup>2</sup>Department of Chemistry, Graduate School of Science and Engineering, Meisei University, Hino, Tokyo 191-8506, Japan and <sup>3</sup>Laboratory of Chromatin Structure and Function, Institute for Quantitative Biosciences, The University of Tokyo, Bunkyo-ku, Tokyo 113-0032, Japan

Received June 18, 2019; Revised September 03, 2019; Editorial Decision September 04, 2019; Accepted September 07, 2019

## ABSTRACT

ATP-DnaA is temporally increased to initiate replication during the cell cycle. Two chromosomal loci, *DARS* (DnaA-reactivating sequences) 1 and 2, promote ATP-DnaA production by nucleotide exchange of ADP-DnaA for timely initiation. ADP-DnaA complexes are constructed on *DARS1* and *DARS2*, bearing a cluster of three DnaA-binding sequences (DnaA boxes I–III), promoting ADP dissociation. Although DnaA has an AAA+ domain, which ordinarily directs construction of oligomers in a head-to-tail manner, DnaA boxes I and II are oriented oppositely. In this study, we constructed a structural model of a head-to-head dimer of DnaA AAA+ domains, and analyzed residues residing on the interface of the model dimer. Gln208 was specifically required for *DARS*-dependent ADP dissociation *in vitro*, and *in vivo* analysis yielded consistent results. Additionally, ADP release from DnaA protomers bound to DnaA boxes I and II was dependent on Gln208 of the DnaA protomers, and DnaA box III-bound DnaA did not release ADP nor require Gln208 for ADP dissociation by *DARS*–DnaA complexes. Based on these and other findings, we propose a model for *DARS*–DnaA complex dynamics during ADP dissociation, and provide novel insight into the regulatory mechanisms of DnaA and the interaction modes of AAA+ domains.

## INTRODUCTION

Initiation of chromosomal replication is rigidly regulated to take place in a timely manner during the cell cycle. In *Escherichia coli*, the initiator protein DnaA plays a crucial role in initiating replication at the *oriC* chromosomal origin (1–3). DnaA is a member of the AAA+ ATPase superfamily, and stably binds ATP or ADP (1,4–7). ATP-DnaA, but not ADP-DnaA, is the active form during initiation. DiaA (DnaA initiator-associating protein) is homotetrameric and binds a few molecules of DnaA, which stimulates ATP-DnaA oligomerization on *oriC* and replication initiation (8,9). The minimal *oriC* region consists of an AT-rich duplex unwinding element (DUE), and DnaA-oligomerization region (DOR) bearing 12 specific DnaA-binding sites (DnaA boxes) with various affinities (Figure 1A) (2,3). Also, integration host factor (IHF), a member of the nucleoid-associated protein family, binds to a specific IHF-binding region (IBR), which partly overlaps the  $\tau$ 1 DnaA box (10). IHF binding to IBR prevents DnaA binding to this site. Also, IHF binding introduces a sharp bend in the DNA, promoting DUE unwinding and replication initiation (11–13).

DnaA consists of four functional domains (Figure 1B, C). Domain I bears specific sites for self-dimerization and interactions with other proteins such as DiaA and DnaB helicase (5,9,14). Domain II is a flexible linker (14,15). Domain III has specific AAA+ motifs for ATP recognition (Walker A/B, Sensor I/II, and Arg-finger) in addition to DnaA-specific motifs for stimulating ATP-DnaA oligomerization (AID-1/2) and DUE unwinding (H/B motifs) (4–6,16–22). Like typical AAA+ proteins, ATP-DnaA is believed to form spiral oligomers on *oriC*, in which Arg-finger

\*To whom correspondence should be addressed. Tel: +81 92 642 6641; Fax: +81 92 642 6646; Email: katayama@phar.kyushu-u.ac.jp

†The authors wish it to be known that, in their opinion, the first two authors should be regarded as joint First Authors.

Present addresses:

Ryo Sugiyama, Asahi Kasei Pharma Co., Tokyo, Japan.

Kazutoshi Kasho, Umeå University, Sweden.

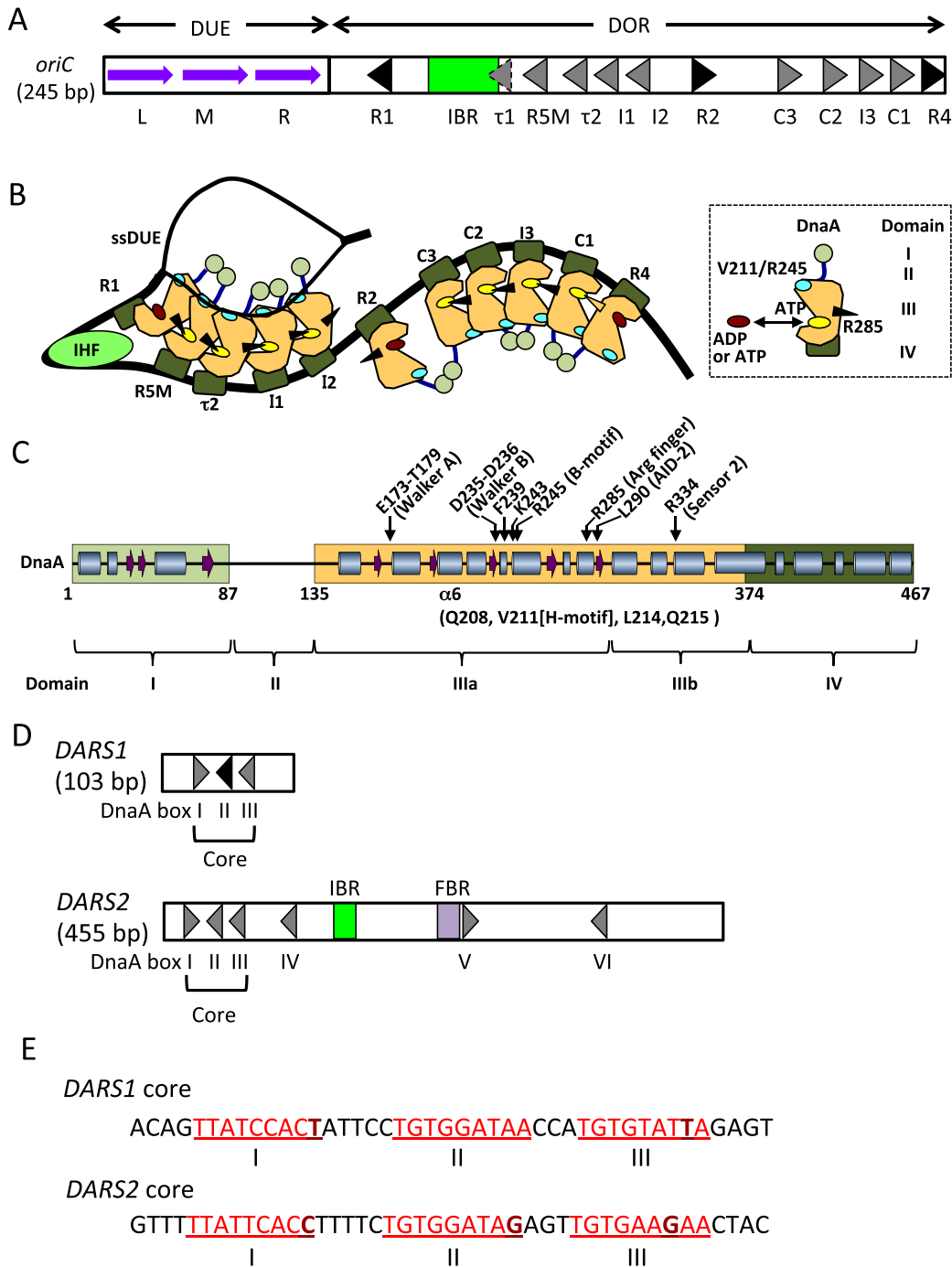


**Figure 1.** Structure of *oriC*, DnaA, the initiation complex, *DARS1*, and *DARS2*. (A) Basic structure of *oriC*. The *oriC* region consists of the duplex unwinding element (DUE) and the DnaA-oligomerization region (DOR). The DUE bears AT-rich 13-mer repeats (L, M, R), while DOR bears a single IHF-binding region (IBR) and 12 DnaA boxes (R1 and 2, R4, R5M,  $\tau$ 1 and 2, I1–3, and C1–3). IBR includes the IHF-binding consensus sequence and partially overlaps DnaA box  $\tau$ 1 (10). Black triangles represent DnaA boxes with the complete consensus sequence (5'-TT[A/T]TNCACA). Dark triangles represent DnaA boxes with the consensus sequence containing one or a few mismatches. These triangles also show the directions of the DnaA box sequences. (B) Model of the initiation complex with unwound DUE (the open complex). DnaA domains are shown (also see panel C). DnaA oligomers are constructed via domain III-domain III interactions in a head-to-tail manner, in which bound ATP interacts with the Arg285 finger motif of the flanking protomer. IHF causes DNA to bend sharply. The T-rich strand of the single-stranded DUE (ssDUE) binds to the Val211 and Arg245 residues of DnaA protomers bound to the R1–I2 region. DiaA is omitted for simplicity. (C) Features of DnaA domains. Domains I–IV are shown with amino acid residue numbers. Domain III is subdivided into IIIa and IIIb. Domain IIIb (residues 296–373) is connected to the IIIa subdomain via a loop (17). The ATP-binding Walker motifs are indicated along with residues relevant to this study. Secondary structures are shown as cylinders for  $\alpha$ -helices and arrows for  $\beta$ -strands.  $\alpha$ 6, the  $\alpha$ 6 helix. (D) Basic structures of *DARS1* and *DARS2*. DnaA boxes are shown as described for panel A. The *DARS* core contains three DnaA boxes, of which two are oriented in a head-to-head manner. *DARS2* has a regulatory region containing an IBR and a Fis-binding region (FBR). (E) Sequences of the *DARS1* and *DARS2* core regions. DnaA box sequences (I, II, and III) are highlighted by red characters and are underlined. DnaA box sequences different from the consensus are indicated by dark red characters.

residue Arg285 interacts with ATP bound to the adjacent protomer, resulting in a head-to-tail DnaA–DnaA interaction (Figure 1B, C) (10,20,23–25). DnaA AID-1 Arg227 and AID-2 Leu290 assist the DnaA–DnaA interaction in the DOR R1-I2, but not significantly in DOR R4-C3 (22). H/B motifs (Val211/Arg245) of DnaA bound to the R1 and R5M sites bind specifically to the T-rich strand of unwound DUE, stabilizing the single-stranded (ss) state, which promotes DnaB helicase loading (Figure 1B, C) (10,13,21,26). Val211 is included in the AAA+ initiator-specific motif (ISM) (4,5,26). Domain IV is a DNA-binding domain for specific recognition of the 9-mer DnaA box, which has the consensus sequence TT(A/T)TNCACA (27,28). In DnaA-DOR complexes, the binding direction of the DnaA protomer relative to this asymmetric sequence has been determined (Figure 1A, B) (24).

The cellular level of ATP-DnaA fluctuates with the peak at the time for replication initiation, which is tightly regulated by negative and positive regulatory systems (3,29–31). DnaA-bound ATP is hydrolyzed and converted to ADP-DnaA by at least two systems, regulatory inactivation of DnaA (RIDA) and *datA*-dependent DnaA-ATP hydrolysis (DDAH), both activated after replication initiation. RIDA is promoted by construction of the complex formed between Hda and the DNA-loaded clamp subunit of DNA polymerase III holoenzyme, which interacts with ATP-DnaA (32,33). DDAH is promoted by the complex formed between IHF and chromosomal locus *datA*, which contains a cluster of DnaA boxes (34,35). IHF-*datA* binding occurs temporally after replication initiation.

By contrast, the DARS system produces ATP-DnaA before replication initiation by promoting nucleotide exchange of ADP-DnaA to ATP-DnaA (36–39). This system is based on at least two chromosomal loci termed *DARS1* and *DARS2* (Figure 1D, E). The two *DARS*s share a highly conserved core region containing three DnaA boxes (I, II, and III) that are essential for nucleotide exchange. ADP-DnaA proteins construct specific dynamic complexes on these loci, which promotes ADP dissociation in the complexes. The resultant apo-DnaA dissociates from the *DARS*-bound complexes and binds ATP, reactivating DnaA molecules (36). *DARS2*, the predominant *DARS* element *in vivo*, is activated in a timely manner by nucleoid proteins Fis and IHF (Figure 1D) (37). *DARS2*-IHF binding occurs temporally before replication initiation.

Whereas many AAA+ proteins are involved in various mechanisms including DNA replication, recombination, and membrane dynamics, they typically form oligomers via a head-to-tail interaction of the AAA+ domains (4,16). However, in the essential cores of *DARS*s, DnaA boxes I and II are oppositely oriented (Figure 1D, E), unlike DnaA boxes II and III, which are oriented in the same direction, like DnaA boxes R1 to I2 and R4 to C3 in the DOR (Figure 1B). DnaA self-associates in a head-to-tail manner at these DnaA boxes facing in the same direction, and the direction of the DnaA boxes appears to play an important role in facilitating the head-to-tail interaction. Although DnaA boxes I and II are essential for the DARS system (36), the fundamental mechanisms by which ADP-DnaA molecules bind to these sites, and possibly interact with each other, largely remain to be explored.

While carrying out this study, a head-to-head dimer structure within the c-di-GMP-bound FleQ AAA+ hexamer from *Pseudomonas aeruginosa* was reported (40). FleQ is a transcriptional regulator that interacts with both a specific enhancer DNA and the sigma factor. Apo-, ADP- and ATP- $\gamma$ -S-bound FleQ hexamers are constructed via typical head-to-tail interactions of AAA+ domains, but when c-di-GMP binds to the hexamer, structural changes occur, resulting in head-to-head dimers of the AAA+ C-terminal subdomains within the AAA+ hexamer. However, these features are largely different from those of *DARS*-DnaA complexes that promote ADP dissociation and do not construct stable hexamers, nor bind c-di-GMP.

In this study, we constructed a structural model of a head-to-head dimer of DnaA AAA+ domains using previous crystal structure analysis (21). In the model, the head-to-head dimer is constructed from AAA+ N-terminal subdomains (domain IIIa; Figure 1C). Based on the model, we analyzed the functions of specific residues predicted to reside on the protein-protein interface, and found that DnaA Gln208 is required for *DARS*-dependent ADP dissociation. *In vivo* analysis using the DnaA Q208A mutant supported the significance of this residue in *DARS* systems, rather than initiation mechanisms at *oriC per se*. Furthermore, we investigated the specific roles of DnaA protomers bound to *DARS1* and found that DnaA bound to DnaA boxes I and II, but not DnaA box III, promotes ADP dissociation dependently on Gln208. In addition, DiaA moderately stimulated *DARS1*-dependent ADP dissociation. Based on these and other findings, we propose a mechanistic model of DnaA–DnaA interactions on *DARS* for dissociating ADP. The results provide novel insight on the regulatory mechanisms of DnaA for replication initiation, and the head-to-head interaction of AAA+ domains.

## MATERIALS AND METHODS

### Bacterial strains, plasmids, and DNA fragments

Strain KH5402-1 (relevant genotype: wild-type [WT] *dnaA*) and its derivative KA451 (*dnaA750::Tn10 rnhA::cat*) have been described previously (19,21), as have derivatives of mini-R plasmids pRRNH (*rnhA*) and pOZ18 (*rnhA*, WT *dnaA*) which bear the *pemI-pemK* stable maintenance system (9,19,22). The pRS1 (*dnaA Q208A*) derivative of pOZ18 was constructed by PCR using mutagenic primers Q208A-1 and Q208A-2 (Supplementary Table S1). The pBR322-derivative pKX11 and pACYC177-derivative pOA61, both of which bear *DARS2*, have been described previously (36). A 1.2 kb DNA fragment carrying a kanamycin resistance gene was amplified using pACYC177 and primers BamHI-kan-f and SphI-kan-r (Supplementary Table S1), digested with *Bam*HI and *Sph*I, and ligated to *Bam*HI-*Sph*I fragments of pBR322 and pKX11, resulting in pBR322-kan and pKX11-kan, respectively. MD1-8 DNA (WT *DARS1*) and its derivatives, as well as Nonsense DNA (MD1-10) bearing a nonsense sequence instead of DnaA boxes I–III (Supplementary Table S1), were constructed by annealing synthetic DNA with complementary sequences. The Nonsense DNA sequence, which excludes DnaA-specific binding, was analyzed previously (10,24,27).

### DnaA overproduction and purification

Plasmids for overproducing mutant DnaA protein were derivatives of pKA234, described previously (41). Mutations were introduced into pKA234 using mutagenic primer pairs Q208A-1 and Q208A-2, and Q215A-1 and Q215A-2 (Supplementary Table S1), resulting in pKA234-Q208A and pKA234-Q215A, respectively. Plasmids pKA234-L214R and pKA234-F239A have been previously described (21,42). Overproduction and purification of DnaA proteins were performed as previously described (21,24), as was expression and purification of DnaA V211A and DnaA L290A (21,22).

### ADP dissociation assay

The ADP dissociation assay was performed essentially as described previously (36,37). Briefly, [<sup>3</sup>H]ADP-DnaA was prepared by incubation of apo-DnaA on ice for 15 min in buffer N (50 mM HEPES-KOH pH 7.6, 2.5 mM magnesium acetate, 0.3 mM EDTA, 7 mM dithiothreitol, 20% v/v glycerol, 0.007% v/v Triton X-100) containing 3 μM [<sup>3</sup>H]ADP. When *DARS1* or chimeric *DARS1* was used, the resultant [<sup>3</sup>H]ADP-DnaA (2 pmol) was incubated in 25 μL of dissociation buffer (20 mM Tris-HCl pH 7.5, 100 mM potassium glutamate, 10 mM magnesium acetate, 2 mM ATP, 8 mM dithiothreitol, 100 μg/mL bovine serum albumin) containing 150 ng of poly(dI-dC) and the indicated amounts of *DARS1* or chimeric *DARS1*. DnaA-bound [<sup>3</sup>H]ADP was recovered on nitrocellulose filters and analyzed using a liquid scintillation counter. When *DARS2* was analyzed, the indicated amounts of *DARS2* plasmid pOA61 and 50 fmol each of IHF and Fis were similarly incubated in the absence of *DARS1*. Where indicated, DiaA (0.25 pmol as tetramer, 1 pmol as monomer) was also co-incubated.

### In vitro oriC replication assay

The *in vitro oriC* replication assay was performed essentially as previously described (9,35,43). Briefly, reaction mixtures (25 μL) contained crude replicative extract prepared from strain WM433 (*dnaA203*), M13KEW101 *oriC* plasmid RF I (200 ng; 600 pmol as nucleotide), rNTPs, dNTPs including [ $\alpha$ -<sup>32</sup>P]dATP and DnaA.

### Electrophoretic mobility shift assay (EMSA)

EMSA experiments were essentially performed as described previously (10,24,37). Briefly, DNA fragments (50 nM) were incubated at 30°C for 10 min in 10 μL of GS buffer (20 mM HEPES-KOH pH 7.6, 100 mM potassium chloride, 20 mM magnesium acetate, 1 mM EDTA, 8 mM dithiothreitol, 100 μg/mL bovine serum albumin, 10% glycerol) containing ADP-DnaA and 50 ng of λ phage DNA as a competitor, followed by 6% polyacrylamide gel electrophoresis (PAGE) at 100 V for 85 min at room temperature in Tris-borate buffer. DnaA was visualized using GelStar staining.

### Flow cytometry analysis

These experiments were essentially performed as described previously (8,10,37). Briefly, cells were grown exponentially

for at least ten generations at 37°C in LB medium. Portions of the cultures were withdrawn for analysis of cell mass (cell size) and other portions were further incubated for four hours in the presence of rifampicin and cefalexin, followed by DNA staining with SYTOX Green and analysis with a FACS Calibur flow cytometer.

## RESULTS

### Structural model of the putative head-to-head DnaA complex

Unlike DnaA boxes on *oriC*, the opposite orientation of DnaA boxes I and II in *DARS1* and *DARS2* suggests that a head-to-head interaction by DnaA molecules occurs at these sites (Figure 1D, E). Given that ADP dissociation basically takes place even with truncated DnaA bearing only domains III and IV (36), DnaA domain III regions bearing AAA+ motifs likely interact with each other to form the predicted head-to-head homodimer. Notably, we previously observed a head-to-head orientation in a crystal structure of an ADP-bound DnaA domain III from the hyperthermophile *Thermotoga maritima* (21; PDB 2Z4R). In this structure, the two DnaA molecules are closely associated with each other, primarily through the α6 helix residing on the N-terminal subdomain (domain IIIa) of the conserved AAA+ domain (Figure 1C). Distance between the C-terminal regions of the monomers in the model complex was 6.5–9 nm which corresponds to the length of 19–26 bp dsDNA (Supplementary Figure S1). Considering that 9-bp DnaA boxes I and II are separated by 5-bp space and that domain IV is connected with domain III via a short flexible linker, this distance could be reasonable in allowing a head-to-head dimer formation of the DnaA molecules. We therefore focused our attention on the amino acid residues that constitute the monomer-monomer interface, and investigated the biological significance of the corresponding residues in *Escherichia coli* DnaA, using a homology model of the *E. coli* DnaA domain III head-to-head homodimer (Figure 2A).

### Residues exposed at the interface of the putative head-to-head complex

We examined the DnaA–DnaA interface in the model, and searched for amino acid residues that may play important roles in the head-to-head interaction. Gln208, Val211, Leu214, Gln215, Phe239 and Lys243 were identified as potential candidates, all of which are exposed at the interface of the head-to-head complex in the model structure (Figure 2A and Supplementary Figure S1). A model of the head-to-tail dimer of DnaA domain III suggests that these residues are not present on the interacting surface of the complex (21) (Figure 2B). Among these residues, DnaA V211A and DnaA K243A inhibit DUE unwinding (21), while Val211 (H-motif or ISM) is crucial for ssDUE binding, and K243A is suggested to cause intrinsic conformational changes in ATP-DnaA oligomers constructed on *oriC* DNA.

### Affinity of mutant DnaA proteins for ADP

DnaA proteins bearing Q208A, L214R, Q215A or F239A, as well as WT DnaA, were purified, and only Leu, a relatively small residue, was substituted with Arg bearing a large

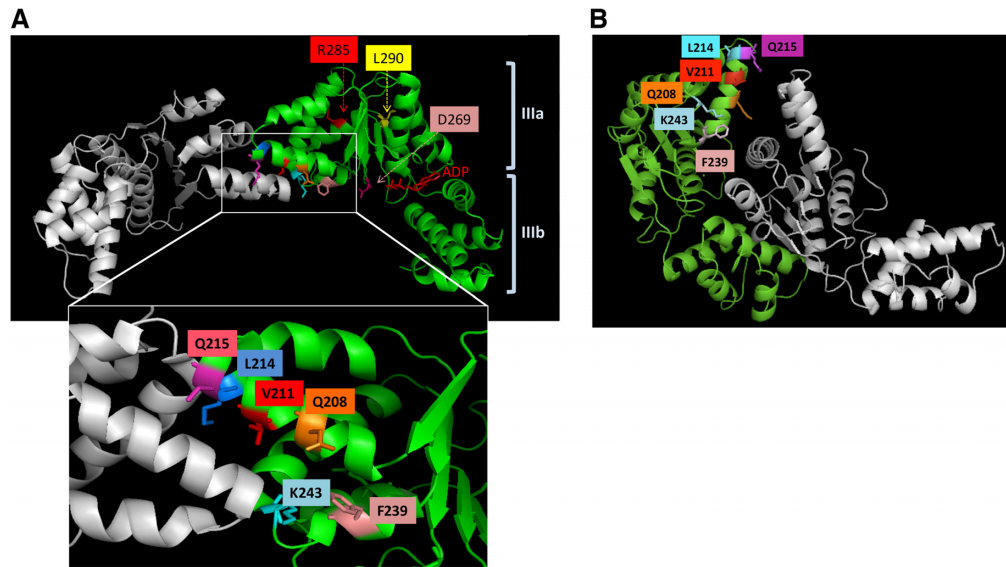


**Figure 2.** Structural model for the head-to-head dimer of DnaA domain III (AAA+ domain). (A) Homology model of the head-to-head dimer of *E. coli* DnaA AAA+ domain III. The crystal structure of the head-to-head dimer of *T. maritima* DnaA AAA+ domain III (21; PDB 2Z4R) was used as a template for homology modeling with an analyzing software MOLFEAT. The overall protein structure is shown in ribbon representation, with different colors for each structurally identical protomer. The monomer-monomer interface is enlarged (*insert*). Residues positioned at the monomer-monomer interface are shown as sticks and colored differently, as are functionally important residues. ADP is also shown in stick representation. The nucleotide-binding pocket is located at the boundary of AAA+ N-terminal and C-terminal subdomains IIIa and IIIb. The same model is shown also in space filling representation (Supplementary Figure S1). (B) Homology model of the head-to-tail dimer of *E. coli* DnaA AAA+ domains. The overall protein structure and residues residing at the monomer-monomer interface are similarly shown (22; PDB 3R8F).

side chain. Filter retention assays showed that the affinities of DnaA Q208A, L214R and Q215A for ADP were comparable to those of WT DnaA (Supplementary Table S2). DnaA F239A appeared to exhibit slightly impaired ADP binding. The flanking residue of Phe239 is another Phe, and the bulky side chains of Phe239 and Phe240 are located only two residues away from the Walker B motif (Asp235–Asp236; Figure 1C). Thus, the F239A substitution may indirectly affect the structure of this motif. DnaA V211A and DnaA K243A have been purified previously with the intact affinity for ADP (21).

#### DnaA Q208A displays impaired ADP dissociation but is active in initiation

To analyze responses to *DARS*, we used reconstituted systems of *DARS1*- and *DARS2*-dependent ADP dissociation of DnaA that included a 70 bp *DARS1* fragment or a 455 bp *DARS2* fragment supporting full ADP dissociation activity (36,37). First, to select specific mutants we used *DARS1*, a simpler system than *DARS2*. ADP-bound DnaA proteins were incubated with *DARS1* DNA, then subjected to filter retention assays. Compared with WT DnaA, DnaA Q208A displayed considerable inhibition in ADP dissociation (Figure 3A); 25 fmol of *DARS1* dissociated ~90% of ADP from WT DnaA, but only ~40% from DnaA Q208A. We previously reported that DnaA L290A is inactive in *DARS2*-dependent ADP dissociation (37). The present data showed that this residue is also crucial for *DARS1* (Figure 3A). By contrast, ADP dissociation activities of DnaA V211A, L214R, and Q215A were essentially sustained (Figure 3B). DnaA F239A and DnaA K243A showed moderate inhibition, suggesting that these residues might play a stimulatory

role in ADP dissociation. As mentioned above (Supplementary Table S2), DnaA F239A could partially alter the intact structure of the nucleotide-binding pocket, causing indirect inhibition of ADP dissociation.

Based on these results, we further analyzed DnaA Q208A using a reconstituted *DARS2* system including IHF and Fis (37). DnaA Q208A displayed moderately impaired ADP dissociation (Figure 3C), consistent with the response to *DARS1*. In addition, we analyzed this mutant using an *in vitro oriC* replication system using a crude replicative extract. Whereas ADP forms of WT DnaA and DnaA Q208A were inactive, ATP forms of the two proteins were fully active (Figure 3D, E). These results demonstrate the specific importance of the Gln208 residue in ADP dissociation by *DARS* systems, and are essentially consistent with the head-to-head complex model (Figure 2A).

#### DiaA diminishes DnaA Q208 activity in ADP dissociation

DiaA has a high affinity for DnaA molecules, and thereby stimulates assembly of DnaA molecules on *oriC* (8,9). This protein forms a homotetramer, and each protomer bears a specific binding site (including DiaA Leu190) for DnaA domain I (8). Binding of the DiaA tetramer to multiple DnaA molecules stimulates the cooperative binding of DnaA molecules on the *oriC* low-affinity DnaA boxes (9). DiaA itself does not substantially bind DNA or nucleotides. In cells, DiaA might affect the function of *DARS*s in addition to *oriC*. While DnaA domains I and II are basically dispensable for *DARS1*-dependent ADP dissociation, the presence of those moderately stimulates the ADP dissociation (37). DnaA domain I bears weak activity to stimulate self-oligomerization (45). Thus, we analyzed *DARS*-dependent

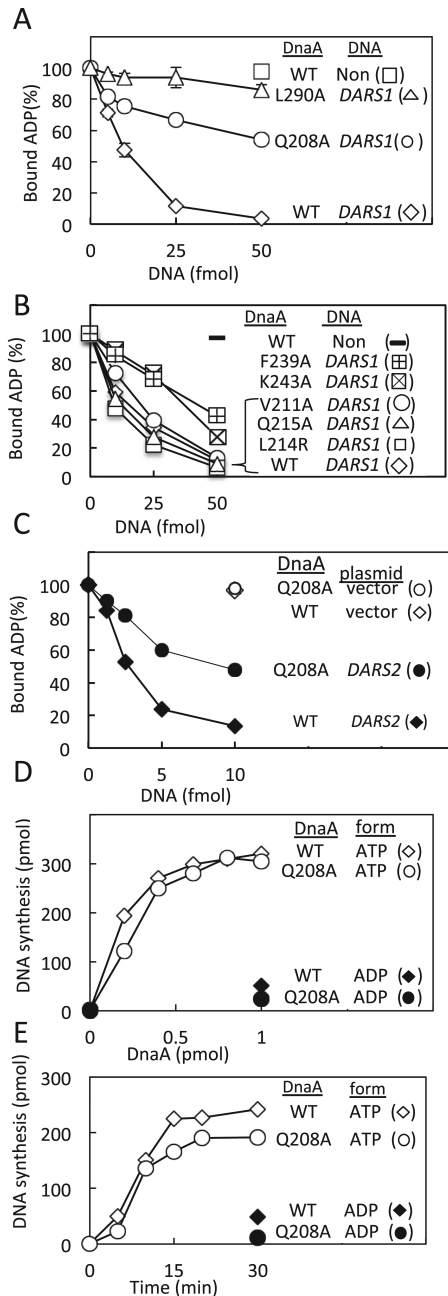


**Figure 3.** ADP dissociation activities of mutant DnaA proteins. (A and B) Activities of *DARS1*. [<sup>3</sup>H]ADP-bound forms of WT and mutant DnaA (2 pmol) were incubated for 15 min at 30°C with the 70 bp MD1–8 DNA including the *DARS1* core (*DARS1*) or the 70 bp Nonsense DNA excluding the *DARS1* core (Non). The amount of DnaA-bound ADP was assessed by a nitrocellulose filter retention assay, and the proportions (%) of the amounts present in the absence of DNA are plotted. Experiments were performed at least twice, and averages with standard deviations (SDs) are shown with error bars. (C) Activities of *DARS2*. [<sup>3</sup>H]ADP-bound forms of WT and DnaA Q208A (2 pmol) were incubated for 15 min at 30°C with pOA61 DNA including the *DARS2* (*DARS2*) or empty plasmid (vector) in the presence of IHF and Fis. The amount of DnaA-bound ADP was similarly assessed. (D and E) Replication initiation activity. *In vitro* complementation assays were performed using a plasmid bearing *oriC* (200 ng, 600 pmol as nucleotide) and a crude extract prepared from a *dnaA* mutant strain (WM433) containing all replication proteins except DnaA. ATP and ADP forms of WT and Q208A DnaA were incubated at 30°C for 20 min (D) or various durations (E). For time-course experiments (E), 1 pmol of DnaA was used for each reaction.

ADP dissociation activities of WT and mutant DnaAs in the presence of DiaA (Figure 4).

First, the ADP form of WT DnaA was incubated with WT DiaA or DiaA L190A that is defective for DnaA binding. Unlike DiaA L190A, WT DiaA moderately stimulated ADP dissociation; whereas 50% ADP dissociation required ~20 pmol of *DARS1* without DiaA, ~10 pmol of *DARS1* was sufficient in the presence of DiaA (Figure 4A and Supplementary Figure S2A). The inactivity of DiaA L190A indicates that this stimulation is dependent on specific DnaA–DiaA binding. Analogous to the case for *oriC*, this stimulation might be due to enhanced assembly of DnaA molecules on *DARS1* by DiaA.

Second, similar analysis of the ADP form of DnaA Q208A indicated that the residual activity of ADP dissociation of DnaA Q208A was diminished by DiaA, resulting in severe inactivity (Figure 4B). This might be because the rate of DnaA assembly is important for construction of a functional DnaA assembly on *DARS1*, and an enhanced assembly rate may negatively impact the residual functional assembly of DnaA Q208A. Alternatively, DiaA may interact weakly with DnaA domain III or IV, thereby affecting the complex structure of DnaA assembly on *DARS1*, which could have positive and negative effects on WT DnaA and DnaA Q208A, respectively.

Third, when DnaA L290A, which is defective in the *DARS2* function (37), was similarly analyzed, full inhibition of ADP dissociation remained, even in the presence of DiaA (Figure 4C). This suggests that DnaA Leu290 sustains structural changes essential for the function of both *DARS1* and *DARS2* (see Discussion).

Fourth, similar analysis was performed using a *DARS2* reconstitution system with ADP forms of WT DnaA or DnaA Q208A (Figure 4D). ADP dissociation activity of WT DnaA was basically similar in the presence or absence of DiaA, although DiaA might slightly stimulate the activity. Unlike the case for *DARS1*, the *DARS2* reconstitution system included IHF and Fis, which enhances DnaA assembly (37), and could reduce the effect of DiaA on WT DnaA. By contrast, the residual activity of ADP dissociation by DnaA Q208A was diminished by DiaA, resulting in severe inhibition, consistent with the results obtained for *DARS1*. This suggests that DnaA Gln208 plays a similar role in *DARS1* and *DARS2* DnaA complexes.

Fifth, we extended the analysis using *DARS1* and DnaA V211A, L214R, Q215A and F239A (Figure 4E–H). Like WT DnaA, these mutant DnaAs were stimulated in ADP dissociation by DiaA.

### DnaA Q208A is active *in vivo* in initiation at *oriC* but is impaired in reactivation at *DARS*

After establishing the specific significance of DnaA Gln208 for DARS systems *in vitro*, we analyzed the *in vivo* significance. To this end, we first analyzed replication initiation activity using plasmid complementation tests with *dnaA::Tn10 rnhA::cat* mutant cells. The *rnhA::cat* sequence activates alternative origins outside *oriC*, allowing chromosomal replication in a *dnaA*-independent manner and slow growth of cells (doubling time ~100 min) (44). The WT *dnaA* or *dnaA Q208A* gene was inserted into a low copy

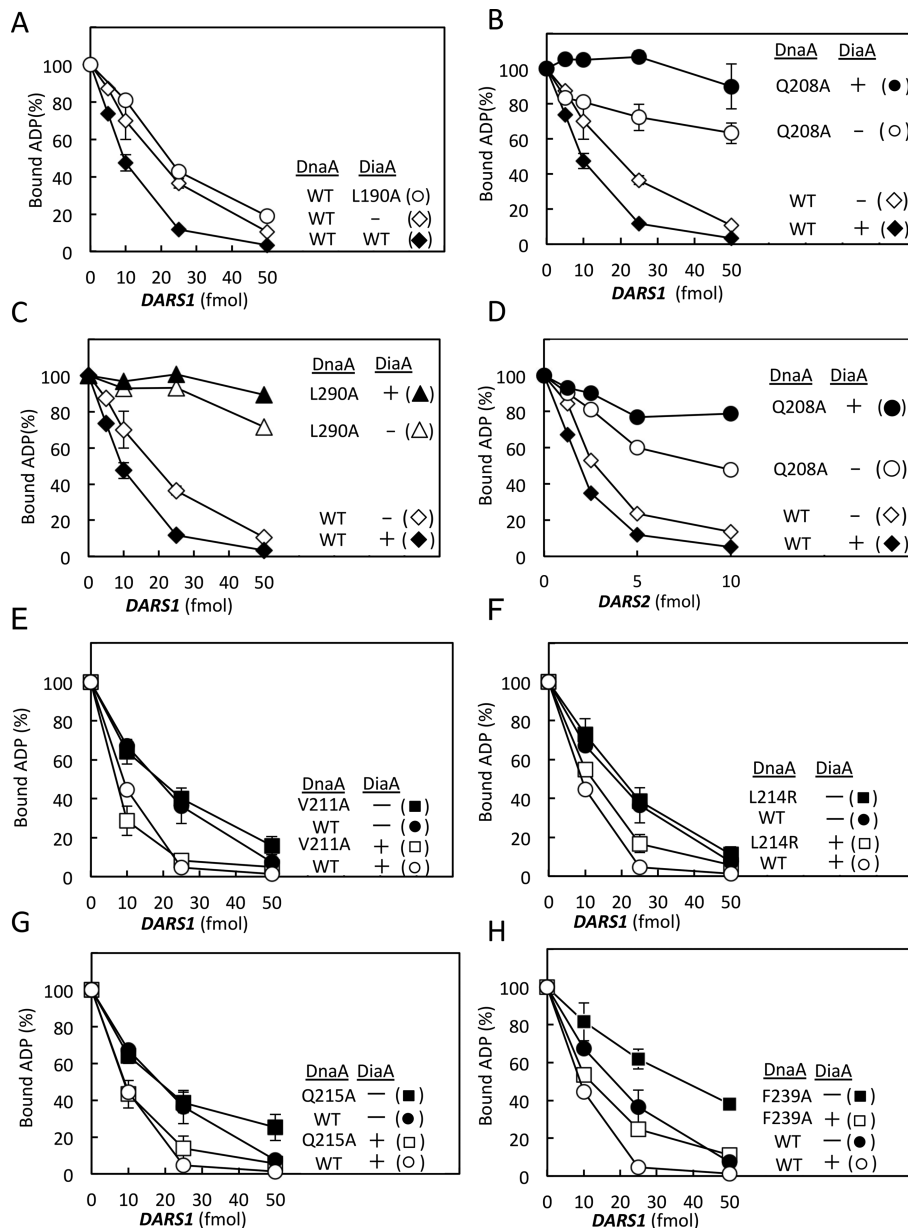


**Figure 4.** ADP dissociation activities of DnaA proteins in the presence of DiaA. (A–C) Activities of WT DnaA, DnaA Q208A, and L290A with *DARS1* in the presence of DiaA. Experiments were performed as described for Figure 3A and B except for the addition of DiaA (0.25 pmol as tetramer, 1 pmol as monomer). DiaA does not directly bind DNA or ADP. These experiments were performed at the same time using WT DnaA and for visibility, the data are shown separately using the identical data of WT DnaA with or without DiaA in each panel. (D) Activities of WT DnaA and DnaA Q208A with *DARS2* in the presence of DiaA. Experiments were performed as described for Figure 3C except for the addition of DiaA (0.25 pmol as tetramer). (E–H) Activities of other DnaA mutants with *DARS1* in the presence of DiaA. Experiments were performed at the same time as described for panels A–C using the indicated DnaAs. For visibility, the data are shown separately in each panel using the identical data of WT DnaA. For all panels, at least two independent experiments were carried out, and mean values are plotted with SD error bars (some SDs are too small to be shown).

number mini-R plasmid bearing the *rnhA* gene (pRRNH). These plasmids (pOZ18 for WT *dnaA*, pRS1 for *dnaA Q208A*) and the pRRNH vector were introduced into a WT *dnaA* strain, and cells were incubated at 30°C for 22 h, and the number of visible colonies was counted. WT *dnaA* cells were transformed with three plasmids at a comparable ef-

iciency, although transformation of pRS1 (*dnaA Q208A*) might be slightly less efficient (Table 1).

Next, these plasmids were introduced into *dnaA::Tn10 rnhA::cat* cells. Since *dnaA::Tn10 rnhA::cat* cells grow slowly, cells complemented with WT *dnaA* could form visible colonies within 22 h under these conditions (19,21). In-

**Table 1.** DnaA Q208A is active in replication initiation *in vivo*

Strain	Relevant genotype		mini-R- <i>rnhA</i> plasmid	<i>dnaA</i> allele on plasmid	Colony formation efficiency ( $\times 10^5$ / $\mu\text{g}$ DNA)
	<i>rnhA</i>	<i>dnaA</i>			
KH5402-1	WT	WT	pOZ18	WT	1.0
	WT	WT	pRS1	Q208A	0.70
	WT	WT	vector	none	1.0
KA451	:: <i>cat</i>	::Tn10	pOZ18	WT	1.1
	:: <i>cat</i>	::Tn10	pRS1	Q208A	0.90
	:: <i>cat</i>	::Tn10	vector	none	$<1.0 \times 10^{-3}$

Cells of the wild-type (WT) *dnaA* strain (KH5402-1) and the *dnaA rnhA* double mutant (KA451) were transformed with mini-R plasmid derivatives (10 ng) harboring only WT *rnhA* (pRRNH vector), WT *rnhA*, and WT *dnaA* (pOZ18), or WT *rnhA* and *dnaA* Q208A (Q208A; pRS1). Transformed cells were incubated on LB agar plates containing 100  $\mu\text{g}/\text{mL}$  ampicillin at 30°C for 22 h, and visible colonies were counted.

roduction of the pRRNH vector did not stimulate growth, resulting in a severely reduced number of colonies (Table 1). However, introduction of pOZ18 bearing WT *dnaA* stimulated the growth of cells by activating *oriC*, resulting in much higher transformation efficiency (and hence colony formation), as previously reported (19,21). Similar activation was shown for pRS1 bearing *dnaA* Q208A. In addition, we analyzed the DnaA expression level in transformed cells using immunoblot analysis (Supplementary Figure S3A). DnaA levels in cells bearing pOZ18 (WT *dnaA*) were similar to those in cells bearing pRS1 (*dnaA* Q208A). These results suggest that DnaA Q208A also activates replication initiation at *oriC* *in vivo*.

To analyze the *in vivo* role of Gln208 in the DARS system, we used a pBR322-derived multicopy plasmid bearing *DARS2*. Introduction of this plasmid into cells severely inhibits colony formation in a manner dependent on *oriC* (36). In this case, oversupply of *DARS2* most likely causes over-activation of DnaA and severe over-initiation of replication, resulting in inhibition of cell growth. Consistent with these previous results, when a pBR322 derivative bearing *DARS2* (pKX11-kan) was introduced into cells expressing WT *dnaA*, colony formation was severely inhibited (Table 2). By contrast, when the *DARS2* plasmid was introduced into cells expressing *dnaA* Q208A but not WT *dnaA*, colony formation was fully sustained (Table 2). Given that DnaA Q208A is essentially active for initiation (Table 1), these results support the idea that DnaA Gln208 is fundamentally instrumental in reactivation by *DARS2* *in vivo*.

In addition, we performed flow cytometry analysis of *dnaA::Tn10* cells bearing pOZ18 (WT *dnaA*) or pRS1 (*dnaA* Q208A), which were used for experiments of Table 1. Cells were grown exponentially, and portions of the cultures were further incubated in the presence of cefalexin and rifampicin for run-out replication of the entire chromosomes (8,10,37). The resultant number of chromosomes per cell (determined by flow cytometry) corresponds to the number of *oriC* copies at the time of drug addition, thereby indicating activity of replication initiation in cells. In those cells bearing WT *dnaA*, the eight-chromosomes peak predominated with a minor peak for four chromosomes (Supplementary Figure S3B). Additional minor peaks for five and six chromosomes indicate asynchronous initiations, likely due to expression of *dnaA* from the mini-R plasmid. In those cells bearing *dnaA* Q208A, the four-chromosomes

peak, rather than the eight-chromosomes peak, predominated, and peaks for five and six chromosomes were enhanced. These results are consistent with the aforementioned results.

#### DnaA Q208A assembly on *DARS* sites in the presence and absence of DiaA

To analyze the role of DnaA Gln208 in DnaA-*DARS* interactions, we performed EMSA experiments under various conditions. When WT ADP-DnaA and the 70 bp *DARS1* fragment were used, four discrete complexes were detected, depending on the amount of ADP-DnaA, and WT apo-DnaA was inefficient for formation of Complexes II–IV (Figure 5A), consistent with our previous data (36). In addition to the *DARS* core bearing three crucial DnaA boxes, we found a degenerated DnaA box sequence flanking DnaA box III within the 70 bp *DARS1* fragment (Supplementary Figure S4). Substitution of the sequence (defined as DnaA box III') with a nonsense sequence lacking specific affinity for DnaA prevented formation of Complex IV, but not Complexes I–III. However, ADP dissociation activity was almost fully sustained with DnaA box III'-substituted *DARS1*, which suggests that DnaA box III' and formation of Complex IV are largely dispensable for ADP dissociation activity (Supplementary Figure S4).

When ADP-DnaA Q208A was similarly analyzed, Complexes I–III were formed at a level similar to WT ADP-DnaA (Figure 5A). These results suggest that functional DnaA assemblies of ADP-DnaA Q208A molecules are largely intact.

When ADP-DnaA L290A was similarly analyzed, Complexes I and II were formed at a level similar to WT ADP-DnaA, but Complex III was decreased slightly (Figure 5A). These results suggest that Complexes I and II of ADP-DnaA L290A molecules are stable, but higher complexes are not very stable. Our previous analysis indicated that DnaA L290A assembly on *DARS2* was unstable, even for Complexes I and II (37). This difference is reasonable because DnaA box II is a complete consensus sequence for *DARS1* and has a single mismatch for *DARS2* (Figure 1E). Stability of *DARS2*-DnaA complexes is likely more dependent on DnaA–DnaA interactions than is stability of *DARS1*-DnaA complexes.

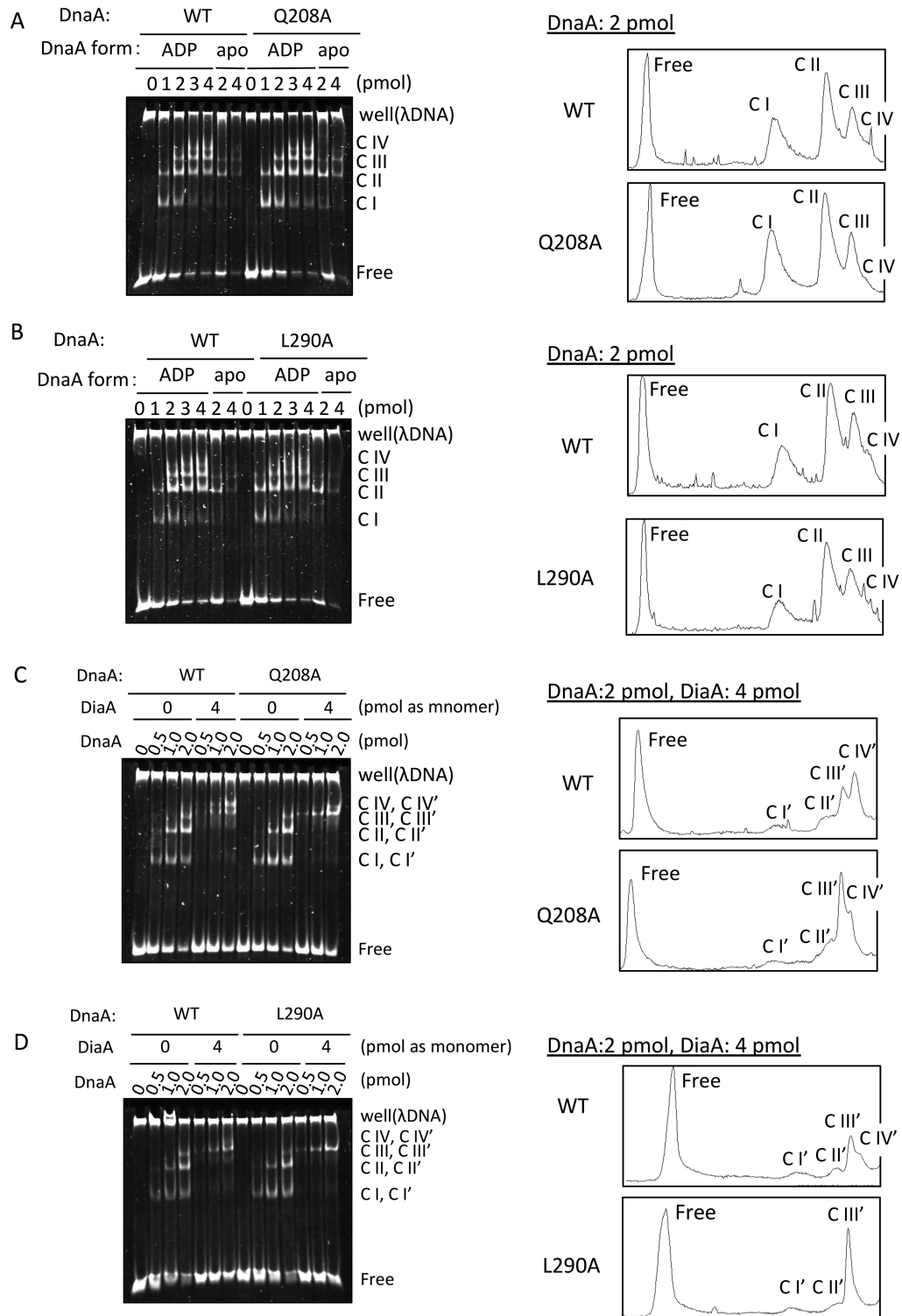


**Figure 5.** EMSA experiments using *DARS1*. (A and B) ADP-bound and apo forms of WT DnaA and DnaA Q208A (A) or DnaA L290A (B) were incubated at 30°C for 5 min with MD1-8 DNA (0.40 pmol), followed by EMSA analysis using 6% PAGE. *Left*, Gel image. *Right*, Intensity plot derived from scanning EMSA data obtained using 2 pmol of DnaA. Free, Protein-free DNA; C I–C IV, Complex I–IV.  $\lambda$  phage DNA was used as a competitor. (C and D) Proteins were similarly incubated in the presence of DiaA and analyzed. Data are also presented similarly, except that data obtained using 2 pmol of DnaA and 4 pmol (as monomer) of DiaA were scanned. In addition, migrating positions of complexes formed in the presence of DiaA (Complexes I'–IV') are labeled as C I'–C IV'. As differences in positions of those and C I–C IV are slight, those complexes are labeled collectively in these panels. For details, see Supplementary Figure S2B.

**Table 2.** Inhibition of cell growth by *DARS2* oversupply is suppressed in *dnaA Q208A* cells

1st plasmid bearing WT <i>rnhA</i>	Plasmid			Colony formation efficiency ( $\times 10^4/\mu\text{g DNA}$ )
	<i>dnaA</i> allele	2nd plasmid	<i>DARS2</i>	
pOZ18	WT	pBR322-kan	–	1.1
		pKX11-kan	+	$<1.6 \times 10^{-3}$
pRS1	<i>Q208A</i>	pBR322-kan	–	1.1
		pKX11-kan	+	1.0

Cells of the *dnaA::Tn10 rnhA::cat* double mutant (KA451) bearing Amp-resistant mini-R plasmid derivative pOZ18 (WT *rnhA* and WT *dnaA*) or pRS1 (WT *rnhA* and *dnaA Q208A*) (1st plasmid) were transformed with Kan-resistant pBR322 derivative (pKX11-kan or pBR322-kan) with (+) or without (–) *DARS2* (2nd plasmid). Portions of transformed cells were incubated on LB agar plates containing 50  $\mu\text{g}/\text{mL}$  kanamycin and 50  $\mu\text{g}/\text{mL}$  ampicillin at 37°C for 22 h, and visible colonies were counted.

EMSA experiments were also performed in the presence of DiaA. Formation of higher complexes (putative Complexes III and IV) of WT ADP-DnaA was stimulated by DiaA (Figure 5C, D), basically consistent with the functional stimulation with *DARS1* (Figure 4A) as well as the role for DiaA in *oriC*. Slight shift up of the bands corresponding to Complexes I–IV was detected depending on DiaA, and those were indicated as Complexes I'–IV' (Figure 5C, D and Supplementary Figure S2B). Although the numbers of DnaA and DiaA molecules in these complexes have not been determined, ADP dissociation experiments suggest that these complexes respectively include DnaA molecules corresponding to Complexes I–IV. Retardation of the migration rates by DiaA in electrophoresis was slight, which would be due to enhanced migration by acidic nature (theoretical *pI* of 5.28) of DiaA contrast to basic nature (theoretical *pI* of 8.77) of DnaA. Addition of DiaA L190A, a DnaA binding-defective mutant, did not substantially change the band patterns in EMSA (Supplementary Figure S2B). Formation of Complex IV was only faint or not detected in the absence of DiaA because of the limited amounts of DnaA. Even for DnaA Q208A and DnaA L290A, formation of Complex III' was stimulated by DiaA compared with WT DnaA, but formation of Complex IV' was not. These results are consistent with those in the absence of DiaA, and suggest that *DARS1* assemblies of DnaA Q208A and DnaA L290A are not fully intact, although overall assemblies on the *DARS* core DnaA boxes I–III are constructed. DnaA–DnaA interaction modes and/or local structures of DnaA–*DARS1* complexes might be altered by the Q208A and L290A mutations.

Addition of DiaA moderately impeded the decrease of the DnaA-free DNA levels (Figure 5C, D). Considering that a DiaA homotetramer stably binds multiple DnaA molecules, free diffusion of each DnaA molecule might be restricted, decreasing the chance to encounter the ligand DNA compared to DiaA-free DnaA monomers under the present conditions.

#### DnaA molecules arranged in head-to-head interactions dissociate ADP

To analyze the specific function of DnaA protomers bound to the *DARS* core, we used chimeric DnaA (chiDnaA) consisting of *E. coli* DnaA domains I–III and *Thermotoga maritima* DnaA domain IV (10,24) (Figure 6A). *T. maritima*

DnaA specifically binds to a sequence (*TmaDnaA* box) different from the *E. coli* DnaA box sequence with a comparable affinity (46), and similarly chiDnaA binds specifically to *TmaDnaA* box, but not the *E. coli* DnaA box (10,24). We separately introduced *TmaDnaA* box into the equivalent position of DnaA boxes I, II, and III (Figure 6B), and the functions of these chimeric *DARS1* derivatives (*DARS1* TmaI–III) were assessed in the presence of *E. coli* DnaA and chiDnaA. Although the consensus sequence of *TmaDnaA* box is 12 mer (AAACCTACCACC) according to sequence analysis (46), previous experiments assessing functional initiation complexes using chiDnaA and *oriC* bearing *TmaDnaA* box suggest that the 5' side of the 9 mer of the *TmaDnaA* box consensus sequence (AAACCTACC) corresponds to the position of the *E. coli* 9-mer DnaA box consensus sequence (TT[A/T]TNCACA) (10,24). Additionally, when DnaA boxes I–III were substituted with *TmaDnaA* box at different positions and ADP dissociation activities were assessed, similar specificity was observed for *TmaDnaA* box (Supplementary Figure S5). These results are consistent with the fact that spaces between DnaA boxes are highly conserved in *DARS1*, *DARS2*, and predicted *DARS*-candidate sequences in various bacterial species (36). Based on these results, we used optimal *DARS1* derivatives (*DARS1* TmaI–III) for further experiments.

First, *E. coli* [<sup>3</sup>H]ADP-DnaA and ADP-chiDnaA were incubated with *DARS1* TmaI–III (Figure 6B–D), and [<sup>3</sup>H]ADP was efficiently dissociated from DnaA when *DARS1* TmaIII was used, whereas *DARS1* TmaI and *DARS1* TmaII promoted moderate [<sup>3</sup>H]ADP dissociation. These results suggest that DnaA bound to DnaA boxes I and II efficiently dissociates ADP, while DnaA bound to DnaA box III does not. When chiDnaA was used, higher amounts of *DARS1* derivatives were required for ADP dissociation compared with WT DnaA and WT *DARS1*, possibly due to retarded turnover rates of DnaA molecules per *DARS1* in the chiDnaA system.

Second, *E. coli* ADP-DnaA and [<sup>3</sup>H]ADP-chiDnaA were incubated with *DARS1* TmaI–III (Figure 6E, F), and [<sup>3</sup>H]ADP dissociation was barely detected when *DARS1* TmaIII was used, whereas *DARS1* TmaI efficiently promoted [<sup>3</sup>H]ADP dissociation, and *DARS1* TmaII also promoted [<sup>3</sup>H]ADP dissociation with moderate efficiency. These results are consistent with the aforementioned proposal that DnaA binding to boxes I and II releases ADP but binding to box III does not.

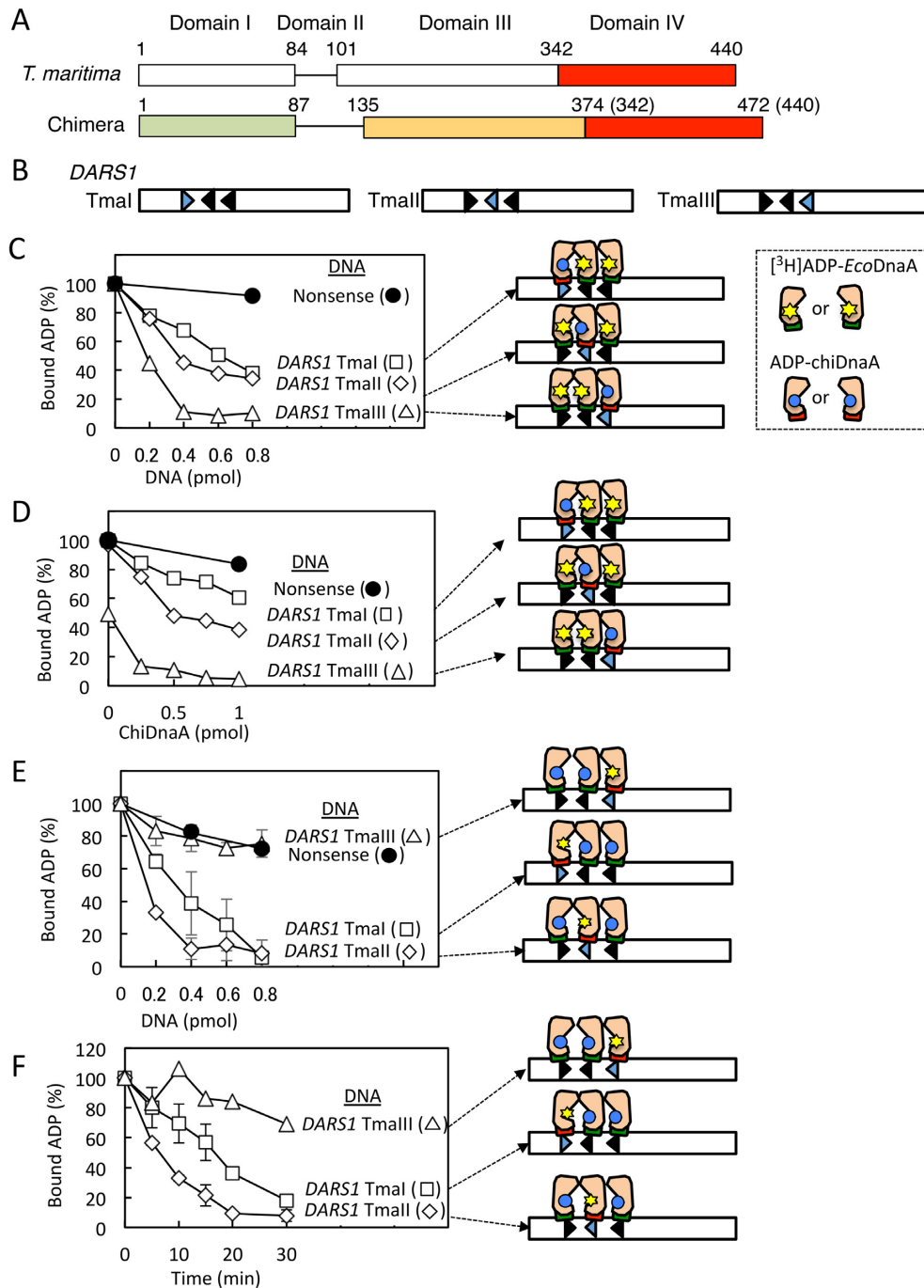


**Figure 6.** Analysis of the specific role of the DnaA protomer using chiDnaA. (A) Schematic representation of the chiDnaA structure. *T. maritima* DnaA and ChiDnaA domains are shown with the amino acid residue numbers. ChiDnaA consists of *E. coli* DnaA domains I–III and *T. maritima* DnaA domain IV (10,24). (B) Schematic representation of chimeric *DARS1* with *E. coli* and *T. maritima* DnaA boxes. *E. coli* DnaA box I, II or III (black triangles) was replaced with *T. maritima* DnaA box (blue triangles), resulting in *DARS1* TmaI, *DARS1* TmaII, and *DARS1* TmaIII, respectively. Sequences are shown in Supplementary Figure S5. (C) [<sup>3</sup>H]ADP-*EcoDnaA* dissociation assay using various DNA concentrations. [<sup>3</sup>H]ADP-*EcoDnaA* (2 pmol) and non-radioactive ADP-chiDnaA (1 pmol) were co-incubated at 30°C for 15 min with the indicated amounts of chimeric *DARS1* TmaI–III or Nonsense DNA excluding DnaA boxes, then subjected to nitrocellulose filter retention assay (Left). Potential DnaA complexes are also illustrated (Right). Only DnaA domains III and IV are shown. Domain IV is colored green for *EcoDnaA* (Eco) and red for chiDnaA (Chi). Similar illustrations are also shown for panels D–F. (D) [<sup>3</sup>H]ADP-*EcoDnaA* dissociation assay using various *DARS1* TmaI–III concentrations. Similar experiments were performed using 0.4 pmol of the indicated DNA, [<sup>3</sup>H]ADP-*EcoDnaA* (2 pmol), and non-radioactive ADP-chiDnaA (0–1 pmol). (E) [<sup>3</sup>H]ADP-chiDnaA dissociation assay. Similar experiments were performed using various amounts of the indicated DNA, non-radioactive ADP-*EcoDnaA* (2 pmol), and [<sup>3</sup>H]ADP-chiDnaA (1 pmol). Data averaged from at least two independent experiments are plotted using mean values and SD error bars. (F) Time course of [<sup>3</sup>H]ADP-chiDnaA dissociation. Similar experiments were performed using 0.4 pmol of chimeric *DARS1* TmaI–III, non-radioactive ADP-*EcoDnaA* (2 pmol), and [<sup>3</sup>H]ADP-chiDnaA (1 pmol). Data averaged from at least two independent experiments are plotted using mean values and SD error bars.

In addition, DnaA assemblies on *DARSI* TmaI–III were assessed by EMSA experiments (Supplementary Figure S6). *DARSI* TmaIII formed Complex III with *E. coli* DnaA less efficiently than WT *DARSI*, and formation of Complex IV was severely inhibited. Formation of Complexes III–IV might be caused by enhancement of non-specific DNA binding of DnaA by cooperative binding processes. However, formation of these complexes was efficiently promoted in the presence of chiDnaA. These results suggest that DnaA complexes were constructed even on *DARSI* TmaIII in the presence of both *E. coli* DnaA and chiDnaA, which further implies that DnaA bound to box III does not dissociate ADP. Similar results were also obtained for *DARSI* TmaI (Supplementary Figure S6). Higher complexes of *DARSI* TmaII including chiDnaA also were formed but were moderately unstable (Supplementary Figure S6). However, this instability in EMSA experiments would not be functionally very significant in that the activity in ADP dissociation was comparable between *DARSI* TmaI and *DARSI* TmaII (Figure 6).

### DnaA Gln208 is instrumental for head-to-head interactions of DnaA

To explore the roles of Gln208 and Leu290 in the DnaA protomers, we further analyzed the reconstituted systems using *E. coli* mutant DnaA, chiDnaA, and *DARSI* derivatives bearing TmaDnaA box. First, *DARSI* TmaIII was incubated with ADP-chiDnaA in addition to the [<sup>3</sup>H]ADP form of *E. coli* WT DnaA, DnaA Q208A, or DnaA L290A (Figure 7A and Supplementary Figure S7). In this system, *E. coli* DnaA should bind to DnaA boxes I and II. In contrast to *E. coli* WT DnaA, DnaA Q208A was impaired in ADP dissociation, supporting the importance of these residues in the head-to-head interaction of DnaA protomers bound to DnaA boxes I and II. Also, DnaA L290A was impaired in ADP dissociation (also see below).

Second, similar experiments were performed using *DARSI* TmaII (Figure 7B and Supplementary Figure S7). In this system, *E. coli* DnaA should bind to DnaA boxes I and III. Unlike the case with *DARSI* TmaIII, ADP dissociation was sustained even for DnaA Q208A. This suggests that ADP dissociation is inhibited only when both DnaA protomers bound to DnaA boxes I and II lose the Gln208 residue. DnaA L290A was impaired in ADP dissociation, including with *DARSI* TmaIII.

Third, similar experiments were performed using *DARSI* TmaI (Figure 7C and Supplementary Figure S7). ADP dissociation of DnaA Q208A was sustained, consistent with the proposed role for this residue. DnaA L290A was inactive in ADP dissociation, including with *DARSI* TmaII. Taken together, the results for DnaA L290A suggest that this residue is important for structural changes of DnaA complex bound to DnaA boxes I and II, rather than head-to-tail interactions between DnaA protomers in the *DARSI* system.

## DISCUSSION

In this study, based on a structural model of a head-to-head dimer of DnaA AAA+ domains, we analyzed the roles

of specific residues residing at the interface of the modeled dimer in ADP dissociation by the DARS system, and revealed that Gln208 is crucial for the reaction. The DnaA Q208A mutant essentially sustained activity for replication initiation from *oriC* *in vitro* and *in vivo*. Further experiments using chimeric DnaA and *DARS* derivatives indicated that DnaA protomers bound to *DARS* DnaA boxes I and II, rather than the box III-bound DnaA, predominantly released ADP, and ADP dissociation was inhibited when Gln208 residues of both DnaA protomers were substituted. Furthermore, we found that DnaA-interacting protein DiaA stimulates *DARSI*-dependent ADP dissociation from WT DnaA, which inversely exaggerated impairment of the DnaA Q208 mutant in *DARSI*-dependent ADP dissociation. Taken together, these results indicate an essential role for head-to-head interactions in the construction of *DARS*s-DnaA complexes competent for ADP dissociation, as well as a second role for DiaA in sustaining timely initiation by stimulating the DARS system. However, we do not exclude the possibility that other structures of DnaA AAA+ head-to-head dimers may also be consistent with the mutant data.

In the *DARSI* core region, DnaA box II has a complete consensus sequence. Based on this, it is reasonable to presume that, during DnaA assembly, DnaA binding to box II is more efficient than to box I or III (Figure 8). Next, the box II-bound DnaA would recruit the additional DnaA molecules to boxes I and III via head-to-head and head-to-tail interactions with DnaA AAA+ domain III respectively. If DnaA box III' is present, another DnaA molecule would be recruited, but this is not a prerequisite for DnaA-ADP dissociation activity. Interactions involving Gln208 in the head-to-head DnaA dimer are essential for the ADP dissociation function. In addition, DnaA Phe239 and Lys243, both residing at Gln208-flanking sites in the tertiary structure model (Figure 2), could assist in the functional head-to-head interaction of AAA+ domain III (Figure 3A). At least one of the two bonds involving Gln208 between monomers is required for functional structural changes during ADP dissociation. In addition, cooperative processes in DnaA assembly on *DARSI* would be enhanced by DiaA.

The head-to-head interaction of the two DnaA AAA+ domains via Gln208 might cause structural changes in the domain that adversely affect the structure of the nucleotide-binding pocket, abolishing ADP-binding activity (Figure 8). The nucleotide-binding pocket is surrounded by AAA+ subdomains IIIa and IIIb in the tertiary structure, and these subdomains are linked via a short loop (Figures 1C and 2). For example, in DnaA molecules bound to boxes I and II, the head-to-head interaction promoted by AAA+ subdomain IIIa bearing Gln208 could swivel the subdomains, expanding the space within the nucleotide-binding pocket (Figure 8). Consistently, a recent structural study using cryo-electron microscopy and an AAA+ protein construct with head-to-tail oligomerization suggests that interaction of an effector protein allosterically induces structural changes in the AAA+ protein, expanding the space within the nucleotide-binding pocket, resulting in ADP dissociation (47).

*DARSI*-DnaA complexes are indicated to require Leu290 for ADP dissociation activity (Figures 3 and 7).

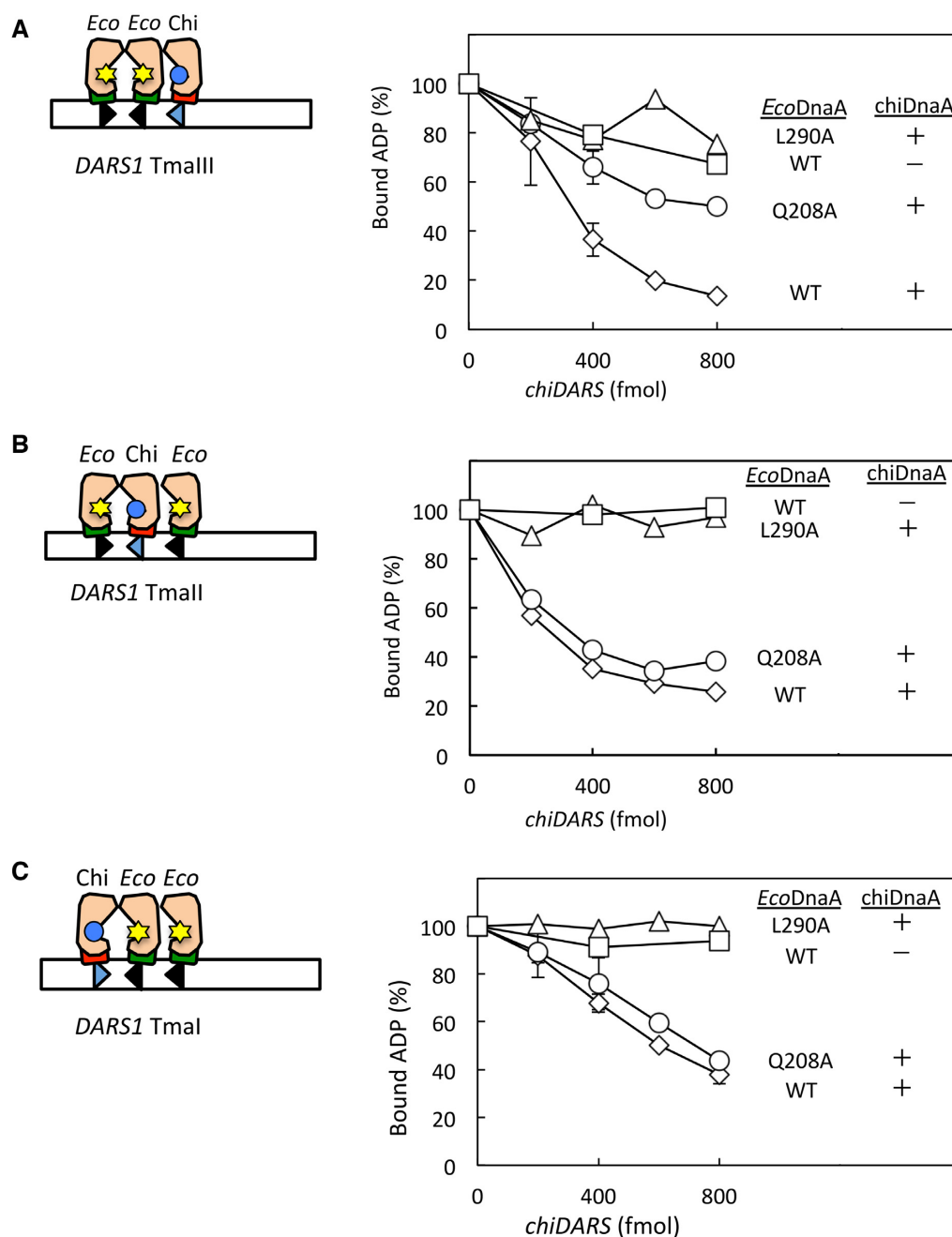


**Figure 7.** Role of Gln208 in head-to-head DnaA dimers.  $[^3\text{H}]$ ADP dissociation assay using *DARS1* TmaI–III.  $[^3\text{H}]$ ADP-*EcoDnaA* (WT, DnaA Q208A, or DnaA L290A; 2 pmol) and non-radioactive ADP-*chiDnaA* (1 pmol) were co-incubated at 30°C for 15 min with *DARS1* TmaIII (A), *DARS1* TmaII (B), or *DARS1* TmaI (C). Predicted DnaA complexes are also illustrated, as shown for Figure 6 (Left).

However, construction of DnaA assemblies was essentially sustained, and was only slightly inhibited with DnaA L290A (Figure 5). This difference suggests that this residue may play an important role in sustaining structural changes in the DnaA complex that support ADP dissociation. This hydrophobic residue resides in the vicinity of AAA+ subdomains IIIa and IIIb, which are linked via a short loop; hence this residue might be important for physically sustaining structural changes around the linker (Figures 1C and 8). In addition to the requirement for Leu290 in DnaAs bound to boxes I and II, there is a possibility that

box III-bound DnaA may also require Leu290 for ADP dissociation by *DARS1*-DnaA complexes. This could be explained by a possibility that structural changes in box III-bound DnaA L290A may adversely affect structural changes in box I- and II-bound DnaA complexes. This idea is consistent with results showing that construction of *DARS1* Complex III was slightly inhibited with DnaA L290A (Figure 5). It should be noted that the structure of DnaA domains III and IV can differ using a short flexible linker between the two domains, which enables swiveling of domain IV (17). Molecular dynamics modeling of *oriC*-

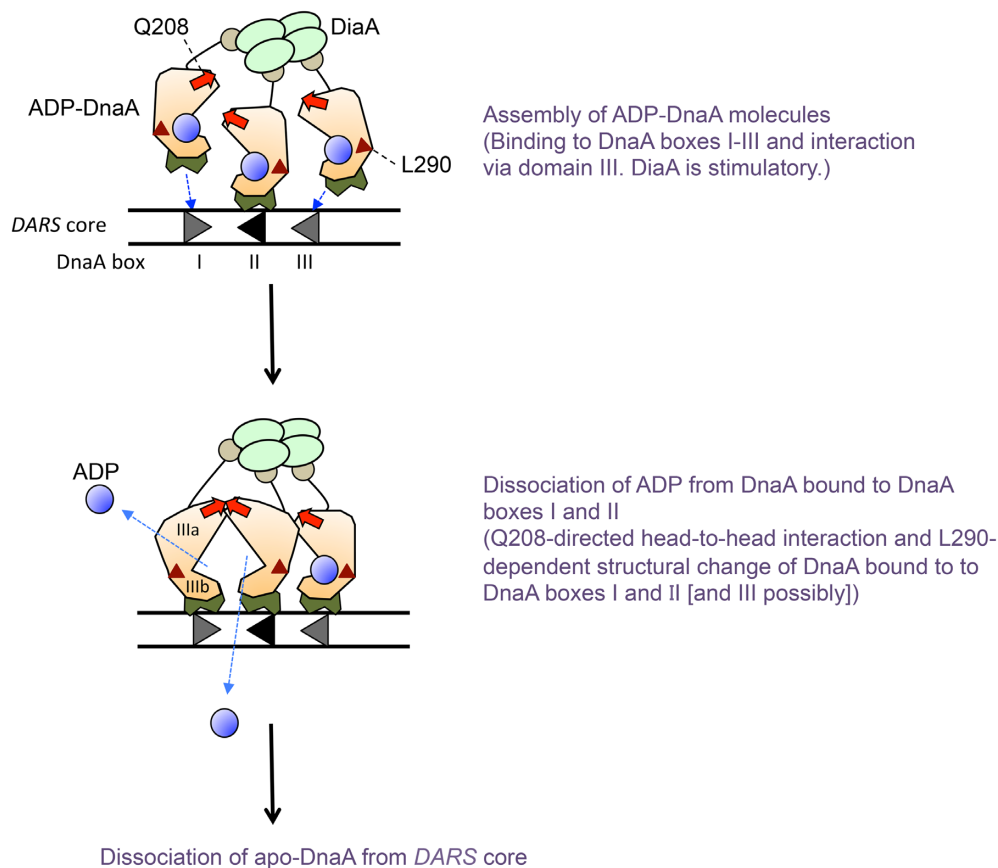


**Figure 8.** Modeling of molecular dynamics in *DARS*-DnaA complexes. A mechanistic model is proposed based on the present and previous studies. *DARS1* DnaA box II includes the complete consensus sequence of the 9-mer DnaA box. We assume that ADP-DnaA binds to this site, recruiting the second and third molecules to DnaA boxes I and III, via head-to-head or head-to-tail interactions of DnaA domain III. The distance between the C-terminal regions of the domain III monomers in the head-to-head dimer might be fitted to that including DnaA boxes I and II and the 5-bp space between the two (Supplementary Figure S1). DiaA homotetramer binding to multiple domain I molecules accelerates these cooperative interaction processes. Interactions between ADP-DnaA molecules promote ADP dissociation from the head-to-head DnaA dimer in a manner dependent on Gln208 in both protomers. This might be caused by induced structural changes in the nucleotide-binding pockets of the head-to-head DnaA dimer, which decreases the affinity for the nucleotide. Leu290 might support these structural changes and might enlarge the relative angle of the boundary between domain III N-terminal and C-terminal subdomains (i.e. domains IIIa and IIIb), relaxing the structure of the nucleotide-binding pocket. Leu290 is located at the domain IIIa C-terminus (Figure 1B). The resulting apo-DnaA dissociates, enabling further interactions of ADP-DnaA molecules, and a new reaction cycle. DnaA domains I (dark circles), II (black lines), III (orange rectangles), and IV (dark green rectangles), ADP (blue circles), Q208 (red arrows), L290 (brown triangles), and DiaA tetramer (pale green circles) are shown.

IHF-DnaA oligomer complexes indicated that each DnaA protomer is structurally different in the complex due to swiveling of domain IV to varying degrees and orientations (25). These various modes for domains III and IV might underlie the possible differences in dependency on Leu290 for complex formation in *DARS1* core DnaA boxes, as well as *oriC* subregions (R1–12 regions vs. R4–C3 regions) (22).

Given these results and the conserved structure of the core region, we can infer that the fundamental mechanisms of DnaA–DnaA interactions and ADP dissociation are likely common between *DARS1* and *DARS2*. In addition, a minor difference between the two systems was apparent since DnaA L290A is less capable of constructing higher oligomers (>Complex II) on *DARS2* (37). This is likely caused by a difference in the affinity of *DARS* core DnaA box II for DnaA (i.e., *DARS1* has a complete DnaA box consensus sequence, but *DARS2* has a sequence with one mismatch; Figure 1E). Also, the *DARS2* DnaA com-

plex is activated for ADP dissociation by binding of Fis and IHF (37). These findings can explain the differences in the dependency on Leu290 in DnaA assembly between *DARS1* and *DARS2*. In addition, the stimulatory effect of DiaA in ADP dissociation was minimum for *DARS2* (Figure 4D). This can also be explained by the previous result, since the *DARS2*-specific factors Fis and IHF play a stimulatory role in DnaA assembly (37). However, detailed roles for these factors in *DARS2* functional mechanisms remain to be elucidated.

Typical AAA+ proteins construct stable homo-oligomers with a ring or spiral configuration that include 5–7 protomers engaging in head-to-tail interactions (4,16). In these complexes, ATP is hydrolyzed, the resulting ADP dissociates, and apo-protomers remain in the complex and bind ATP again to initiate a new reaction cycle. The structures of complexes are altered during nucleotide transfer reactions. Unlike these typical cases, DnaA molecules bound to *DARS*s are released from the complex when ADP dissoci-

ates. Releasing apo-DnaA protomers is crucial for recycling *DARS* elements, and promoting efficient ADP release and reactivation of DnaA proteins, all of which must take place at specific times before replication initiation during the cell cycle. Head-to-head interaction of AAA+ domains, rather than head-to-tail interactions, might be advantageous for constructing dynamic complexes that undergo rapid disassembly and assembly. The DnaA protein and *DARS* elements might have evolved to capitalize on such an advantage.

## SUPPLEMENTARY DATA

Supplementary Data are available at NAR Online.

## ACKNOWLEDGEMENTS

We are grateful to Dr Hironori Kawakami and Dr Yukari Sakiyama for experimental suggestions, and to Kyushu University Research Support Center for shared facilities.

## FUNDING

JSPS KAKENHI funding [JP26291004, JP16H00775, JP17H03656]. Funding for open access charge: JSPS [JP17H03656].

*Conflict of interest statement.* None declared.

## REFERENCES

- Costa, A., Hood, I.V. and Berger, J.M. (2013) Mechanisms for initiating cellular DNA replication. *Annu. Rev. Biochem.*, **82**, 25–54.
- Leonard, A.C. and Grimwade, J.E. (2015) The orisome: structure and function. *Front. Microbiol.*, **6**, 545.
- Katayama, T., Kasho, K. and Kawakami, H. (2017) The DnaA cycle in *Escherichia coli*: Activation, function and inactivation of the initiator protein. *Front. Microbiol.*, **8**, 2496.
- Iyer, L.M., Leipe, D.D., Koonin, E.V. and Aravind, L. (2004) Evolutionary history and higher order classification of AAA+ ATPases. *J. Struct. Biol.*, **146**, 11–31.
- Ozaki, S. and Katayama, T. (2009) DnaA structure, function, and dynamics in the initiation at the chromosomal origin. *Plasmid* **62**, 71–82.
- Kawakami, H. and Katayama, T. (2010) DnaA, ORC, and Cdc6: similarity beyond the domains of life and diversity. *Biochem. Cell Biol.*, **88**, 49–62.
- Kaguni, J.M. (2011) Replication initiation at the *Escherichia coli* chromosomal origin. *Curr. Opin. Chem. Biol.*, **15**, 606–613.
- Keyamura, K., Fujikawa, N., Ishida, T., Ozaki, S., Su'etsugu, M., Fujimitsu, K., Kagawa, W., Yokoyama, S., Kurumizaka, H. and Katayama, T. (2007) The interaction of DiaA and DnaA regulates the replication cycle in *E. coli* by directly promoting ATP DnaA-specific initiation complexes. *Genes Dev.*, **21**, 2083–2099.
- Keyamura, K., Abe, Y., Higashi, M., Ueda, T. and Katayama, T. (2009) DiaA dynamics are coupled with changes in initial origin complexes leading to helicase loading. *J. Biol. Chem.*, **284**, 25038–25050.
- Sakiyama, Y., Kasho, K., Noguchi, Y., Kawakami, H. and Katayama, T. (2017) Regulatory dynamics in the ternary DnaA complex for initiation of chromosomal replication in *Escherichia coli*. *Nucleic Acids Res.*, **45**, 12354–12373.
- Swinger, K.K. and Rice, P.A. (2004) IHF and HU: flexible architects of bent DNA. *Curr. Opin. Struct. Biol.*, **14**, 28–35.
- Hwang, D.S. and Kornberg, A. (1992) Opening of the replication origin of *Escherichia coli* by DnaA protein with protein HU or IHF. *J. Biol. Chem.*, **267**, 23083–23086.
- Ozaki, S. and Katayama, T. (2012) Highly organized DnaA-*oriC* complexes recruit the single-stranded DNA for replication initiation. *Nucleic Acids Res.*, **40**, 1648–1665.
- Abe, Y., Jo, T., Matsuda, Y., Matsunaga, C., Katayama, T. and Ueda, T. (2007) Structure and function of DnaA N-terminal domains: Specific sites and mechanisms in inter-DnaA interaction and in DnaB helicase loading on *oriC*. *J. Biol. Chem.*, **282**, 17816–17827.
- Nozaki, S. and Ogawa, T. (2008) Determination of the minimum domain II size of *Escherichia coli* DnaA protein essential for cell viability. *Microbiology*, **154**, 3379–3384.
- Hanson, P.I. and Whiteheart, S.W. (2005) AAA+ proteins: have engine, will work. *Nat. Rev. Mol. Cell Biol.*, **6**, 519–529.
- Erzberger, J.P., Pirruccello, M. M. and Berger, J.M. (2002) The structure of bacterial DnaA: implications for general mechanisms underlying DNA replication initiation. *EMBO J.*, **21**, 4763–4773.
- Nishida, S., Fujimitsu, K., Sekimizu, K., Ohmura, T., Ueda, T. and Katayama, T. (2002) A nucleotide switch in the *Escherichia coli* DnaA protein initiates chromosomal replication: evidence from a mutant DnaA protein defective in regulatory ATP hydrolysis *in vitro* and *in vivo*. *J. Biol. Chem.*, **277**, 14986–14995.
- Kawakami, H., Ozaki, S., Suzuki, S., Nakamura, K., Senriuchi, T., Su'etsugu, M., Fujimitsu, K. and Katayama, T. (2006) The exceptionally tight affinity of DnaA for ATP/ADP requires a unique aspartic acid residue in the AAA+ sensor I motif. *Mol. Microbiol.*, **62**, 1310–1324.
- Erzberger, J.P., Mott, M.L. and Berger, J.M. (2006) Structural basis for ATP-dependent DnaA assembly and replication-origin remodeling. *Nat. Struct. Mol. Biol.*, **13**, 676–683.
- Ozaki, S., Kawakami, H., Nakamura, K., Fujikawa, N., Kagawa, W., Park, S.-Y., Yokoyama, S., Kurumizaka, H. and Katayama, T. (2008) A common mechanism for the ATP–DnaA-dependent formation of open complexes at the replication origin. *J. Biol. Chem.*, **283**, 8351–8362.
- Ozaki, S., Noguchi, Y., Hayashi, Y., Miyazaki, E. and Katayama, T. (2012) Differentiation of the DnaA-*oriC* subcomplex for DNA unwinding in a replication initiation complex. *J. Biol. Chem.*, **287**, 37458–37471.
- Kawakami, H., Keyamura, K. and Katayama, T. (2005) Formation of an ATPDnaA-specific initiation complex requires DnaA Arginine 285, a conserved motif in the AAA+ protein family. *J. Biol. Chem.*, **280**, 27420–27430.
- Noguchi, Y., Sakiyama, Y., Kawakami, H. and Katayama, T. (2015) The Arg fingers of key DnaA protomers are oriented inward within the replication origin *oriC* and stimulate DnaA subcomplexes in the initiation complex. *J. Biol. Chem.*, **290**, 20295–20312.
- Shimizu, M., Noguchi, Y., Sakiyama, Y., Kawakami, H., Katayama, T. and Takada, S. (2016) Near-atomic structural model for bacterial DNA replication initiation complex and its functional insights. *Proc. Natl. Acad. Sci. U.S.A.*, **113**, E8021–E8030.
- Duderstadt, K.E., Chuang, K. and Berger, J.M. (2011) DNA stretching by bacterial initiators promotes replication origin opening. *Nature*, **478**, 209–213.
- Schaper, S. and Messer, W. (1995) Interaction of the initiator protein DnaA of *Escherichia coli* with its DNA target. *J. Biol. Chem.*, **270**, 17622–17626.
- Fujikawa, N., Kurumizaka, H., Nureki, O., Terada, T., Shirouzu, M., Katayama, T. and Yokoyama, S. (2003) Structural basis of replication origin recognition by the DnaA protein. *Nucleic Acids Res.*, **31**, 2077–2086.
- Katayama, T., Ozaki, S., Keyamura, K. and Fujimitsu, K. (2010) Regulation of the replication cycle: conserved and diverse regulatory systems for DnaA and *oriC*. *Nat. Rev. Microbiol.*, **8**, 163–170.
- Kurokawa, K., Nishida, S., Emoto, A., Sekimizu, K. and Katayama, T. (1999) Replication cycle-coordinated change of the adenine nucleotide-bound forms of DnaA protein in *Escherichia coli*. *EMBO J.*, **18**, 6642–6652.
- Riber, L., Frimodt-Møller, J., Charbon, G. and Løbner-Olesen, A. (2016) Multiple DNA binding proteins contribute to timing of chromosome replication in *E. coli*. *Front. Mol. Biosci.*, **3**, 29.
- Katayama, T., Kubota, T., Kurokawa, K., Crooke, E. and Sekimizu, K. (1998) The initiator function of DnaA protein is negatively regulated by the sliding clamp of the *E. coli* chromosomal replicase. *Cell* **94**, 61–71.
- Kato, J. and Katayama, T. (2001) Hda, a novel DnaA-related protein, regulates the replication cycle in *Escherichia coli*. *EMBO J.*, **20**, 4253–4262.

34. Kitagawa,R., Ozaki,T., Moriya,S. and Ogawa,T. (1998) Negative control of replication initiation by a novel chromosomal locus exhibiting exceptional affinity for *Escherichia coli* DnaA protein. *Genes Dev.*, **12**, 3032–3043.
35. Kasho,K. and Katayama,T. (2013) DnaA binding locus *datA* promotes DnaA-ATP hydrolysis to enable cell cycle-coordinated replication initiation. *Proc. Natl. Acad. Sci. U.S.A.*, **110**, 936–941.
36. Fujimitsu,K., Senriuchi,T. and Katayama,T. (2009) Specific genomic sequences of *E. coli* promote replicational initiation by directly reactivating ADP-DnaA. *Genes Dev.*, **23**, 1221–1233.
37. Kasho,K., Fujimitsu,K., Matoba,T., Oshima,T. and Katayama,T. (2014) Timely binding of IHF and Fis to *DARS2* regulates ATP-DnaA production and replication initiation. *Nucleic Acids Res.*, **42**, 13134–13149.
38. Inoue,Y., Tanaka,H., Kasho,K., Fujimitsu,K., Oshima,T. and Katayama,T. (2016) Chromosomal location of the DnaA-reactivating sequence *DARS2* is important to regulate timely initiation of DNA replication in *Escherichia coli*. *Genes Cells* **21**, 1015–1023.
39. Frimodt-Møller,J., Charbon,G., Krogfelt,K.A. and Løbner-Olesen,A. (2016) DNA replication control is linked to genomic positioning of control regions in *Escherichia coli*. *PLOS Genet.*, **12**, e1006286.
40. Matsuyama,B.Y., Krasteva,P.V., Baraquetd,C., Harwood,C.S., Sondermann,H. and Navarro,M.V.A.S. (2016) Mechanistic insights into c-di-GMP-dependent control of the biofilm regulator FleQ from *Pseudomonas aeruginosa*. *Proc. Natl. Acad. Sci. U.S.A.*, **113**, E209–E218.
41. Kubota,T., Katayama,T., Ito,Y., Mizushima,T. and Sekimizu,K. (1997) Conformational transition of DnaA protein by ATP: structural analysis of DnaA protein, the initiator of *Escherichia coli* chromosome replication. *Biochem. Biophys. Res. Commun.*, **232**, 130–135.
42. Ozaki,S., Noguchi,Y., Nishimura,M. and Katayama,T. (2012). Stable nucleotide binding to DnaA requires a specific glutamic acid residue within the AAA+ box II motif. *J. Struct. Biol.*, **179**, 242–250.
43. Fuller,R.S., Kaguni,J.M. and Kornberg,A. (1981) Enzymatic replication of the origin of the *Escherichia coli* chromosome. *Proc. Natl. Acad. Sci. U.S.A.*, **78**, 7370–7374.
44. Kogoma,T. (1997) Stable DNA replication. Interplay between DNA replication, homologous recombination, and transcription. *Microbiol. Mol. Biol. Rev.*, **61**, 212–238
45. Felczak,M.M., Simmons,L.A. and Kaguni,J.M. (2005). An essential tryptophan of *Escherichia coli* DnaA protein functions in oligomerization at the *E. coli* replication origin. *J. Biol. Chem.*, **280**, 24627–24633.
46. Ozaki,S., Fujimitsu,K., Kurumizaka,H. and Katayama,T. (2006) The DnaA homolog of the hyperthermophilic eubacterium *Thermotoga maritima* forms an open complex with a minimal 149-bp origin region in an ATP-dependent manner. *Genes Cells*, **11**, 425–438
47. Wang,J., Wang,J., Hu,M., Wu,S., Qi,J., Wang,G., Han,Z., Qi,Y., Gao,N., Wang,H.W. *et al.* (2019) Ligand-triggered allosteric ADP release primes a plant NLR complex. *Science*, **364**, eaav5868.